Separable Space-Time Pattern Synthesis for the TechSat21 Space-Based Radar System

Hans Steyskal, John K. Schindler
Air Force Research Laboratory, SNHA
80 Scott Drive
Hanscom AFB, MA 01731, USA
Tel: 781-377-2052, Fax: 781-377-5040, hans.steyskal@hanscom.af.mil

Abstract—The TechSat21 space-based radar employs a cluster of free-floating satellites, each of which transmits its own orthogonal signal and receives all reflected signals. The satellites operate coherently at X-band. The cluster forms essentially a multi-element interferometer with a concomitant large number of grating lobes and significant ground clutter. A novel technique for pattern synthesis in angle-frequency space with thinned arrays, combined with reduced order space-time processing, was presented by us at the 2001 IEEE Aerospace Conference, along with some preliminary results. We now give a full evaluation of this technique and its effectiveness in clutter suppression. [1]

TABLE OF CONTENTS

1. INTRODUCTION

The use of large spatially thinned arrays for space-based radar detection of slowly moving ground targets is considered. The TechSat21 space-based radar concept employs a cluster of free-floating satellites, each transmitting its own orthogonal signal and receiving all reflected signals, similar to the French RIAS system [1]. The satellites operate coherently at X-band (3 cm wavelength). The cluster forms a large, multi-element interferometer with narrow beamwidth and concomitant large number of grating lobes and significant ground clutter. Other approaches to thinned, space based radar antennas [2] have not considered arrays of free-floating satellites.

A novel technique for pattern synthesis in angle-frequency space with thinned arrays was introduced by us at the 2001 IEEE Aerospace Conference [3]. However, at that time, only preliminary results for limited system parameters were available, and several aspects were left open.

In this paper, we first motivate our approach, which is based on a thinned periodic array and a carefully selected pulse repetition frequency, combined with 'separable' (sequential) space-time processing. For an M-element array followed by an N-pulse Doppler filter thus there are M+N degrees of freedom available for signal/clutter optimization. We then evaluate the effectiveness of our separable space-time processing for clutter suppression, and compare it with the effectiveness of fully general space-time processing.

2. BASIC CONSIDERATIONS

Detection of a slowly moving ground target from a moving radar is based on the difference of the Doppler frequencies of the target return and the ground clutter. The situation is depicted in Fig. 1, where the ground clutter ridge $C_{clutter}$ is the return from one range bin illuminated by the antenna main beam and sidelobes. The different angular parts of the range bin generate an extended Doppler spectrum, since they have radial velocities that vary with azimuth angle φ, as seen from the radar. A moving target in the antenna main beam appears as a spike in the angle-Doppler domain. To separate the target return from the clutter ridge clearly requires a narrow antenna main beam and a narrow Doppler filter bandwidth, or equivalently, a minimum aperture dimension A and coherent integration time T. These can be shown to be

$$A \approx \frac{3}{2}\frac{v_{radar}}{v_{target}}\lambda, \qquad T \approx \frac{3}{4}\frac{\lambda}{v_{target}} \tag{1}$$

where v_{target} is the radial target speed, v_{radar} the radar along track speed, and λ the radar wavelength. Sampling the aperture A at $\lambda/2$ spacing leads to a total number of spatial samples (array elements)

$$N_s = 3\frac{v_{radar}}{v_{target}}. \tag{2a}$$

[1] U.S. Government work not protected by U.S. copyright.

Similarly, over the time T, the total number of temporal samples

$$N_T = 3\frac{v_{radar}}{v_{target}}, \qquad (2b)$$

since the minimum temporal sampling rate equals twice the highest Doppler frequency $2\, v_{radar}/\lambda$.

It is interesting to note that the total numbers of spatial and temporal samples are equal, and that they are determined solely by the ratio of v_{radar}/v_{target}, independent of the radar frequency. However, for slowly moving targets viewed from space these numbers are large. For example, a target speed v_{target} = 2.2 m/s (8 km/hour) and a low Earth orbit radar speed v_{radar} = 7500 m/s leads to

$$N_A = N_T = 10^4$$

corresponding to a (linear) array with 10000 elements that generates 10^8 space-time samples at each range sample for unambiguous azimuth-Doppler processing. The narrow beamwidth and long processing times can slow the search rate of such a radar system and the large number of space-time samples present a substantial signal processing requirement. Thus there is a strong motivation for reducing the number of samples, i.e. for spatial and temporal undersampling.

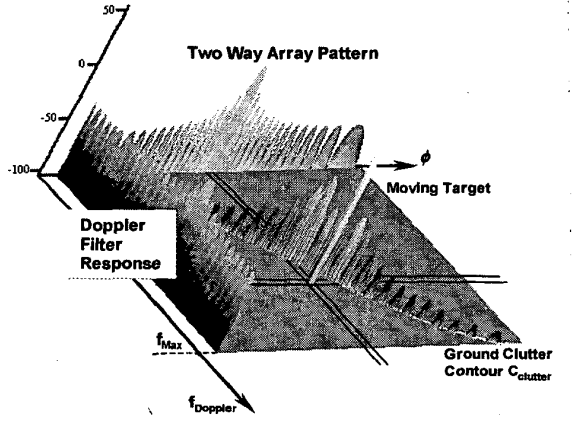

Figure 1 - Target return and ground clutter return in Angle-Doppler space.

A spatially undersampled or thinned array maintains the narrow beamwidth necessary for slow moving target detection but introduces excess clutter associated with the lost sidelobe control. Basically, thinning can be periodic or random, which leads to very different sidelobe structures and received clutter Doppler spectra, as seen in Fig. 2. As reference, the clutter spectrum corresponding to a fully filled array is shown. It decreases monotonically away from the main beam, corresponding to the continuous decrease of the sidelobe envelope. Further shown is the spectrum corresponding to a periodically thinned array, whose grating lobes generate a periodic spectrum. Here the clutter is concentrated to relatively high, narrow spectral bands with low clutter regions between. Finally, there is shown the ensemble average clutter spectrum for a randomly thinned array. The clutter power is concentrated at a Doppler frequency corresponding to the main beam pointing direction with a bandwidth that is comparable to that produced by the fully filled array. Outside the main beam, the power is uniform at a level proportional to $1/N^2$, where N is the number of elements in the array. A single realization of the randomly thinned array is also shown by the dotted curve.

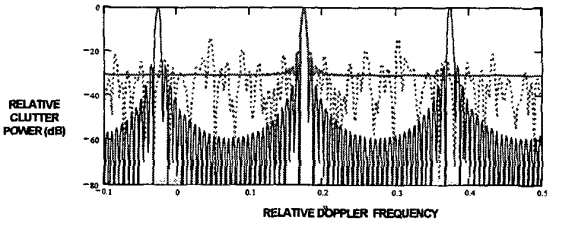

Figure 2 - Clutter Doppler spectrum received with fully filled array and with thinned periodic and thinned random arrays.

The periodically thinned array is preferred since between the harmonic spectral lines, the power spectrum of the clutter is smaller than for the random array, permitting better target detectability. In addition, it is compatible with temporal periodic undersampling of this power spectrum. Selecting a sampling frequency (pulse repetition frequency) related to the harmonic spectral lines results in aliased overlap of the spectral lines, which retains the relatively low clutter power between the spectral lines. Fig. 3 illustrates this point. It shows the power spectrum of a periodically thinned array along with the power transfer function of a 3-pulse binomial canceller, and the resultant uniform residual clutter at the output of the cancellation filter.

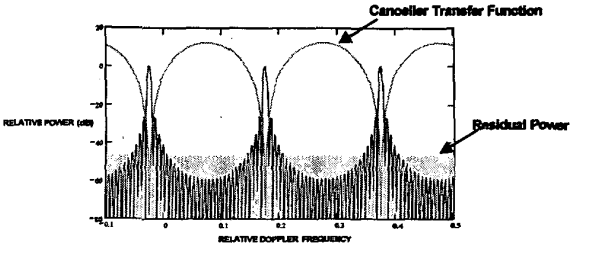

Figure 3 - Incident clutter Doppler spectrum, Doppler filter transfer function and resultant output power spectrum.

The array signal processing considered here involves an array beam former followed by a Doppler filter and is denoted as 'separable' processing, since it performs spatial and temporal processing independently. Figure 4 illustrates this separable processing. It is considerably simpler than

general space-time processing, where each space-time sample is individually weighted and summed.

This basic approach of a thinned periodic array with a 'tuned' pulse repetition frequency (PRF) and separable processing was applied to the TechSat21 radar system.

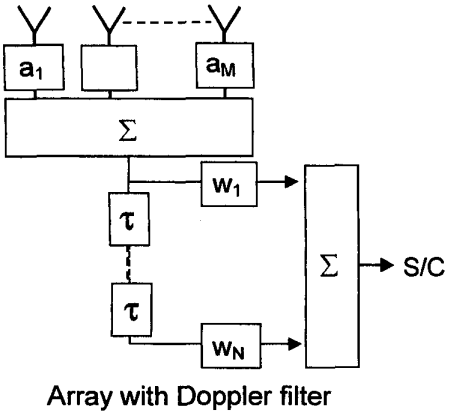

Figure 4 - The array with Doppler filter has M+N degrees of freedom available for Signal/Clutter optimization.

3. APPLICATION TO TECHSAT21

Cluster configurations are governed by orbital mechanics, i.e. Kepler's equations. Linearization for small motions around a reference point in a global circular orbit leads to the Hill equations, derived in 1878, alternatively named Clohessy-Wiltshire equations, who rederived them in 1960 [4]. These equations constrain the satellites to move either linearly along track or to local orbits around the reference point, such that their projections on a vertical plane form 2:1 ellipses.

Our proposed TechSat configuration consists of a vertical, planar 19-element array as shown in Figure 5. The vertical orientation allows looking toward both sides equally well and gives the higest gain at maximum range. The array configuration, with one central element and six elements on each of three concentric 2:1 ellipses, realizes a periodic triangular grid. During each Earth orbit the elements rotate one full cycle along their respective ellipses but maintain a triangular grid (the ellipse major axes remain parallel to the circular orbit). The triangular lattice is the key to our approach since it generates grating lobes that are highly periodic in angle, and, from further analysis, periodic in Doppler spectrum as well.

The rotation of the array around its center, which continuously changes the grating lobe structure, is a complication, since it requires a corresponding 'tuning' of the PRF.

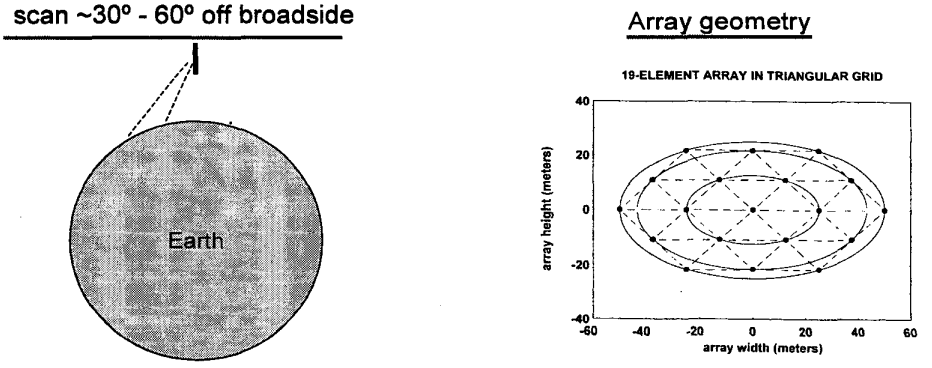

Figure 5 - Proposed TechSat21 array configuration consisting of 19 free floating satellites.

Another complication is due to the curvature and rotation of the Earth. However, since each satellite element is assumed to have a 2m square aperture at X band, only a relatively small angular sector of the Earth is illuminated and the grating lobes and Doppler frequencies experience nearly the same linear shift, as shown by numerical analysis. Figure 6 illustrates the ground clutter power spectrum resulting from the 19-element TechSat21 array viewing the Earth through a conical (constant range) pattern cut. These representative results correspond to a satellite array nominal altitude of 850 km in an orbital plane inclined 70° relative to the equator, with satellites positioned 45° above the equator and with a look down angle of 45°. Even though the array is pointed broadside to the orbital plane, the center frequency of the spectrum is approximately 10 kHz due to Earth rotation. The envelope of the grating lobe pattern is due to the two-way satellite array pattern.

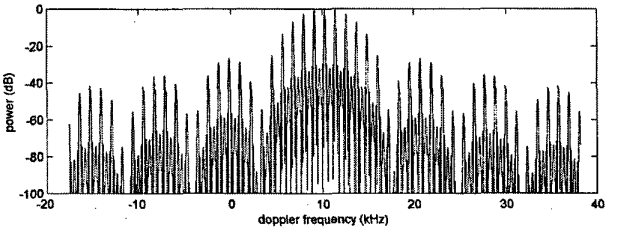

Figure 6 - Array pattern (2-way) in terms of Doppler frequency.

Figure 7 shows the aliased ground clutter spectrum when the PRF of the radar is selected to correspond to the fourth grating lobe of the antenna pattern, f_{rep} = 4640 Hz. There is little spreading of the spectral lines associated with each grating lobe, implying significant periodicity of the array grating lobe Doppler frequencies over the beamwidth of the satellite array pattern. Also, the spectrum between the grating lobes does not decrease monotonically as with a uniformly illuminated linear array. This is due to the effective amplitude modulation imposed by the two dimensional, vertical aperture.

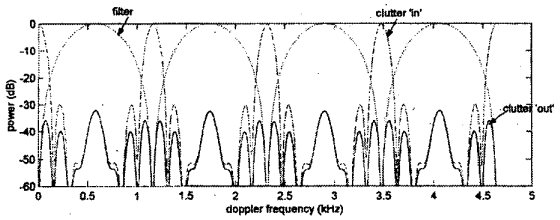

Figure 7 – Clutter suppression with an N-pulse canceller; "filter" is the power transfer function of the canceller; "clutter 'in'" and "clutter 'out'" represent clutter power spectrum at the input and output of the canceller (N=13).

For moving target indication, the clutter spectral lines are suppressed by an N-pulse canceller, implemented simply as a 2, 3 or 4 pulse canceller (i.e. a binomial canceller or cascaded 2 pulse cancellers) depending on the aliased grating lobe bandwidth using desampled radar data. N represents the total number of pulses acquired during a coherent cancellation dwell, with N=13 corresponding to a four pulse canceller implemented with every fourth pulse received. We have managed to reduce the clutter residue to a fairly uniform level across the whole Doppler band, as is illustrated in Fig. 7. The canceller weights were chosen deterministically using only knowledge of the Doppler frequencies and spectral width of the aliased grating lobes but without knowledge of other details of the clutter spectrum at the input.

4. Performance of the Rotating Array

The above examples were all given for the elliptical array at an array rotation angle φ_a=0°, i.e. the situation shown in Fig. 5 with five elements on the major axes of the ellipses. This represents the best periodic case. However, during one Earth orbit, the array rotates 360° around its center and changes its triangular grid and thus its grating lobe structure. Therefore we also evaluated performance for other array rotation angles φ_a, over the range $0 \leq \varphi_a \leq 30°$ in 5° increments, after which the array configuration repeats due to symmetry.

We found that we can always select a basic pulse repetition frequency that leads to signal to clutter (S/C) improvement factors around 25 dB. Fig. 8 shows these improvement factors and the corresponding PRFs that maximize signal to clutter. Here S/C improvement was defined as S/C at the filter output relative to S/C at the single receive element, assuming target Doppler frequency to be uniformly distributed between 0 Hz and PRF, and the filter being a binomial, 5-pulse canceller. Multiples of these basic PRFs give the same result and thus our approach is robust with respect to both array rotation angle and PRF.

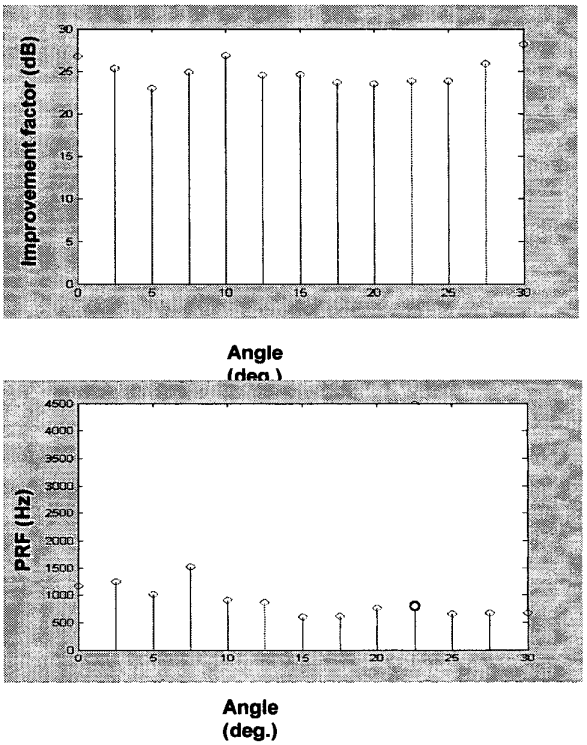

Figure 8 - Signal/Clutter improvement factor vs. array rotation angle (top), and corresponding pulse repetition frequencies (bottom).

5. Optimization of Separable Space-Time Processing

Our proposed approach for separable space-time processing has M receive element weights a_m and N filter weights w_n, (see Fig 4), which in the examples above were chosen corresponding to a maximum gain array, (i.e. a_m=1), and to a classical N-pulse canceller, (i.e. w_n=binomial coefficients), respectively. However, these weights can be chosen so as to maximize the S/C improvement factor. Optimizing either the weights a_n or the weights w_m leads to a ratio of quadratic forms in terms of these weights, which has a well-known maximum solution [5].

We have performed such computations for various filter orders and the array rotation angles, φ_a=0° and φ_a=5°, which represent best and worst cases, respectively. The results are shown in Fig. 9. We note that array optimization is considerably more effective than filter optimization. Also, apparently the N-pulse canceller matches optimum weighting for low filter orders (2-4 pulses) but degrades for

higher orders. This is because the deterministic weights place nulls only over the dominant Doppler lines. Once these first order contributors have been suppressed to a uniform level, additional nulls at these locations will not improve the processing gain. Optimized weights, however, continue to null second order contributors, so performance improves, although slowly.

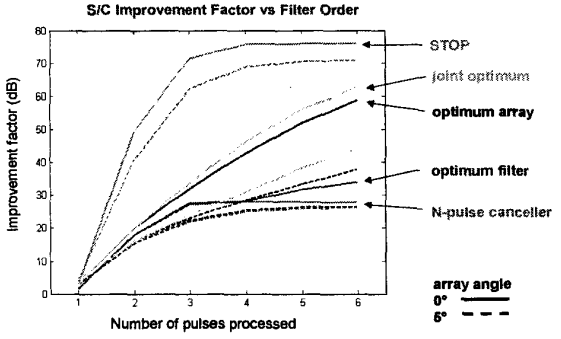

Figure 9 - Signal/Clutter improvement factor vs. filter order for various alternatives of optimization.

A joint optimization of the array and filter weights can be achieved in an iterative fashion by alternatingly optimizing the a_m and w_n. Convergence is rapid and although not guaranteeing a global maximum, it leads to a maximum improvement factor attainable with separable space-time processing. The results shown in Fig. 9 represent only slight improvement over the optimized array with a simple N-pulse canceller.

6. Comparison with General Space-Time Processing

Finally, for reference, we compare separable processing with the ultimate case of space-time optimal processing (STOP), where each array element is followed by an individual Doppler filter. In contrast to separable processing which employs M+N degrees of freedom, STOP employs MxN degrees of freedom. Performing an analysis as before, but now based on the full space-time clutter covariance matrix, leads to the results shown also in Fig. 9. The additional degrees of freedom clearly give superior improvement factors. When the number of pulses exceeds 3, the curves are noise limited.

Our separable approach is critically based on a periodic array and a 'tuned' PRF. An interesting question therefore is, whether the flexibility of general space-time processing can relieve this requirement for array periodicity.

To explore this question, we added random errors to the element location, such that they were distributed uniformly within a square 5 m box in the orbital plane and centered at the desired points, and recomputed the S/C improvement factors, assuming that the errors were known by independent measurements. The results for two sample cases are shown in Fig. 10. Clearly even the general STOP solution benefits from a periodic array lattice.

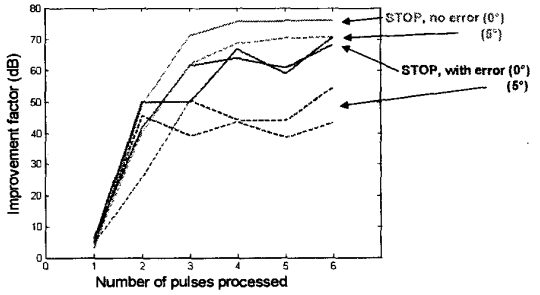

Figure 10 - Comparison of Signal/Clutter improvement factors achievable with a periodic array and array with periodicity spoiled by random but known errors (two realizations).

7. Conclusions

We have considered a 'separable' system architecture for TechSat21, where a planar M-element array is followed by a single N-pulse Doppler filter, and have evaluated some processing alternatives for their effectiveness in clutter suppression. An attractive feature of this architecture is that it allows simple, multi-pulse MTI processing and adaptive antenna pattern control. The limited number of degrees of freedom, M+N, require a relatively low computational load.

General space-time processing offers substantially improved signal/clutter ratios. However, it employs a much larger number of degrees of freedom, MxN, and may be associated with a computational load that is difficult to realize. Synthesis techniques for thinned apertures on transmit and receive, and the trade between performance and processing complexity merit further study.

An interesting conclusion is that a periodic array lattice apparently allows for significantly better clutter suppression than a non-periodic lattice, independent of the particular space-time processing scheme.

Acknowledgements

The US Air Force Office of Scientific Research supported this study under Dr. Arje Nachman. We gratefully acknowledge the contributions to this work of Dr. Robert Mailloux, Dr. Peter Franchi and Dr. Scott Santarelli.

References

[1] Dorey et al: *RIAS, Radar a Impulsion et Antenne Synthetique.* Int'l Conf. on Radar, Paris, Apr. 1989.

[2] J. H. G. Ender: *Spacebased SAR/MTI using Multistatic Satellite Configurations.* EUSAR, Cologne, Germany, June 2002.

[3] H. Steyskal, J. Schindler, P. Franchi, R. Mailloux: *Pattern Synthesis for TechSat21 – A Distributed Space-Based Radar System.* IEEE Aerospace Conference, Big Sky, MT, March 2001.

[4] J.P. Prussing, B. A. Conway: *Orbital Mechanics.* Oxford University Press, 1993.

[5] D.H. Johnson, D.E. Dudgeon: *Array Signal Processing.* Prentice-Hall, 1993.

BIOGRAPHY

Hans Steyskal received the degrees Civ. Ing., Tekn. Lic., and Tekn. Dr. in electrical engineering from the Royal Institute of Technology (KTH), Stockholm, Sweden in 1963, 1970 and 1973, respectively. In 1962, he joined the Swedish National Defence Research Establishment (FOA), where he worked on microwave radiation and scattering problems. In 1980, he gave up his position as Chief, Section for Field and Circuit Theory, and moved permanently to the United States. He now pursues his interests in electromagnetics and applied mathematics at the AFRL Antenna Technology Branch, Hanscom AFB, MA. Since 1996 he is also an Adjunct Professor in Antenna Technology at KTH.

Dr. Steyskal has been a visiting researcher at the Polytechnic U. of New York and the Federal Inst. of Technology, Lausanne, Switzerland. He has served as Associate Editor for the IEEE Transaction on Antennas and Propagation, and is a Fellow of the IEEE.

John K. Schindler received the SB degree from the Massachusetts Institute of Technology and the SM and PhD degrees from Purdue University, all in Electrical Engineering. Prior to his retirement, he was the Director of Electromagnetics and Reliability at the Air Force Rome Laboratory where he directed research and development activities in electromagnetics, solid state electronics and reliability. In addition, he served on a Defense task force to organize and manage the DoD electronics program. He is a lecturer in Electrical Engineering at Northeastern University, teaching graduate courses in radar and digital communications. He has consulted on radar target classification, antenna design and radar cross section measurements. He has been an adjunct Professor of Electrical Engineering at the Air Force Institute of Technology. Dr. Schindler is a Fellow of the IEEE and a recipient of the IEEE Millennium Medal, the Meritorious Civilian Service Award and the Presidential Rank Award of Meritorious Executive.